

Cite this: *Soft Matter*, 2011, **7**, 3234

www.rsc.org/softmatter

PAPER

## Non-Gaussian athermal fluctuations in active gels†

Toshihiro Toyota,<sup>a</sup> David A. Head,<sup>b</sup> Christoph F. Schmidt<sup>c</sup> and Daisuke Mizuno<sup>\*a</sup>

Received 3rd September 2010, Accepted 20th January 2011

DOI: 10.1039/c0sm00925c

Dynamic networks designed to model the cell cytoskeleton can be reconstituted from filamentous actin, the motor protein myosin and a permanent cross-linker. They are driven out of equilibrium when the molecular motors are active. This gives rise to athermal fluctuations that can be recorded by tracking probe particles that are dispersed in the network. We have here probed athermal fluctuations in such “active gels” using video microrheology. We have measured the full distribution of probe displacements, also known as the van Hove correlation function. The dominant influence of thermal or athermal fluctuations can be detected by varying the lag time over which the displacements are measured. We argue that the exponential tails of the distribution derive from single motors close to the probes, and we extract an estimate of the velocity of motor heads along the actin filaments. The distribution exhibits a central Gaussian region which we assume derives from the action of many independent motor proteins far from the probe particles when athermal fluctuations dominate. Recording the whole distribution rather than just the typically measured second moment of probe fluctuations (mean-squared displacement) thus allowed us to differentiate between the effect of individual motors and the collective action of many motors.

### Introduction

Living cells and organisms maintain their activity by continually harvesting external sources of energy. Since the motion of cellular structures under these conditions does not obey the statistics of thermodynamic equilibrium, novel experimental and analytic techniques need to be devised in order to physically describe the “active materials” of nature. Athermal fluctuations violate the fluctuation–dissipation theorem,<sup>1</sup> which links the thermal fluctuation of a given observable to the response of the same observable to an externally applied stimulus.<sup>2,3</sup> Such fluctuations have been recently characterized both in living cells and reconstituted model cytoskeletons using microrheology techniques. The athermal fluctuations of a probe particle were estimated from a comparison of the material’s viscoelastic response measured with active microrheology<sup>4–6</sup> and the total fluctuations of a probe particle measured with passive microrheology.<sup>7–9</sup> Any difference between the results from these two experiments, which were observed at low (*i.e.*, biologically relevant) frequencies, is attributed to athermal fluctuations.<sup>3,5,10</sup>

Although it is intriguing to apply this methodology to living cells,<sup>2,10</sup> their complex intracellular structure and the unspecified origins of forces have prevented the detailed physical interpretation of the observed athermal fluctuations. It is therefore useful to reconstitute the dynamic structures of living cells in a simplified model system, by extracting the essential components of the cellular cytoskeleton and reconstituting them *in vitro*.<sup>11–13</sup> The cytoskeleton is present in most eukaryotic cells, and owes its mechanical integrity to the presence of semi-flexible protein fibers, the most abundant of which, filamentous actin (F-actin), primarily exists beneath the cell membrane in the form of a bundled or cross-linked network. Being actuated by myosin motor proteins, the actin cytoskeleton promotes various cellular processes such as organelle transport, muscle contraction, or the separation of cells in cell division.<sup>11–14</sup> In previous studies, the mechanics of the actin cytoskeleton has been studied mostly in equilibrium.<sup>5,8,15,16</sup> Single molecule techniques have furthermore elucidated the action of motor proteins on single cytoskeletal filaments, out of the cellular environments.<sup>17,18</sup>

In this study, the athermal fluctuations of probe particles dispersed in an “active gel”, composed of a cross-linked actin network with myosin motor proteins, were measured using video microrheology. Under the conditions of our sample preparation, myosin II forms multimeric bipolar clusters *in vitro*. These “mini-filaments” can link different actin filaments and drive them relative to each other (Fig. 1). The non-equilibrium fluctuations in the motion of dispersed probe particles, which are typically much larger than thermal fluctuations, can be easily observed in this active gel at the (long) time-scales accessible to video

<sup>a</sup>Department of Physics, Kyushu University, Higashi-ku, Hakozaki 6-10-1, 812-8581 Fukuoka, Japan. E-mail: mizuno@phys.kyushu-u.ac.jp

<sup>b</sup>Institut für Festkörperforschung, Theorie II, Forschungszentrum Jülich, 52425, Germany

<sup>c</sup>Drittes Physikalisches Institut, Fakultät für Physik, Georg-August-Universität, Göttingen, 37077, Germany

† Electronic supplementary information (ESI) available: See DOI: 10.1039/c0sm00925c

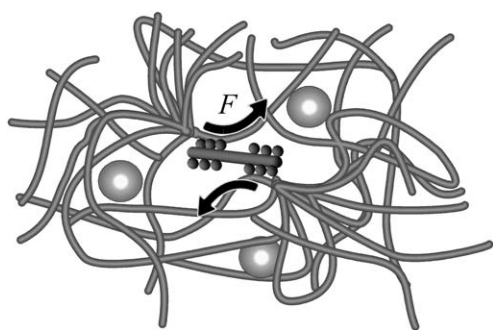


**Fig. 1** Schematic illustration of force generation in an active gel. Here a myosin mini-filament (the bipolar structure at the centre of the drawing) generates relative motion between two actin filaments as shown by the arrows, and thus drives the athermal motion of probe particles (spheres) dispersed in the actin network.

sampling (30 Hz).<sup>3</sup> With video, large athermal fluctuations are stably tracked for times much longer than what is usually doable using laser interferometry.<sup>19</sup> By calculating the distribution of displacements of particles over various lag times ( $\tau = 0.033\text{--}33.3$  s), we obtained both the spatial and temporal characteristics of the non-equilibrium fluctuations. We found that the distribution of athermal fluctuations was not Gaussian, but could be well fitted by a sum of Gaussian-like and exponential functions. We discuss qualitatively how the action of myosin mini-filaments in dynamically responding actin cytoskeletons can explain the spatial distribution and lag-time dependence of athermal fluctuations.

## Results

As schematically shown in Fig. 1, we study the athermal fluctuations driven by myosin motor proteins by observing the motion of probe particles (silica, 1  $\mu\text{m}$  diameter) dispersed in actin networks. In order to maintain a stable network structure under the forces generated by myosin mini-filaments, the actin network was cross-linked using the specific binding between a small amount of biotinylated actin and multivalent neutravidin. Without this cross-linked structure, even weak force generation leads to irreversible collapse of actin networks known as super-precipitation.<sup>20</sup> In Fig. 2B, a typical trajectory of a single probe particle dispersed in the actin/myosin network (*i.e.*, an active gel) is shown and compared with that obtained in a cross-linked actin network without myosin (a passive gel, Fig. 2A). Ballistic motions (*i.e.*, linear trajectories) of probe particles are occasionally observed in active gels, with zero net preferred direction. On the other hand, the trajectories of particles dispersed in passive gels are isotropic and exhibit no ballistic episode. Particles fluctuate purely thermally around their average position. In this elastic, highly cross-linked network, thermal forces can only drive small fluctuations of probe particles, so that the trajectories in active gels are dispersed over a much wider area, as shown in Fig. 2B. Although such trajectories are subject to both thermal and athermal forces, it was found in a prior microrheology study on similar gels<sup>8</sup> that the fluctuation–dissipation theorem was violated at frequencies below  $\sim 10$  Hz, which includes most of the frequency range accessible to video microrheology ( $< 15$  Hz).

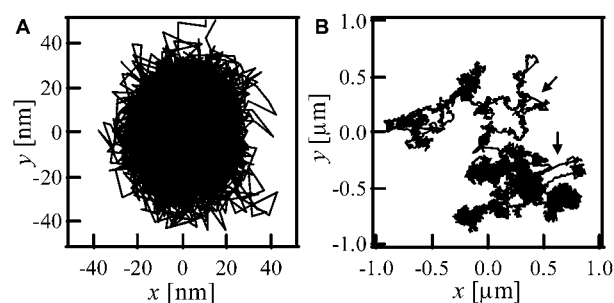


**Fig. 2** (A) A typical trajectory of a silica particle (diameter: 1  $\mu\text{m}$ ) in a cross-linked actin network without myosin (equilibrium state). This trajectory was taken at 30 Hz for about 250 s. (B) A typical trajectory of a silica particle (1  $\mu\text{m}$ ) in an actin–myosin active gel (non-equilibrium state). This trajectory was taken at 30 Hz for about 560 s. Occasional large movements of the particle are indicated by arrows.

This is confirmed by our analysis below, where thermal fluctuations are only important for the highest frequencies observed.

In order to study the detailed statistical properties of athermal fluctuations in active networks, we calculated the ensemble-averaged van Hove correlation function of particle trajectories,  $P(\Delta x(\tau))$  defined as the distribution of particle displacements over a given time lag,  $\tau$ , represented as

$$P(\Delta x(\tau)), \Delta x(\tau) = x(t + \tau) - x(t) \quad (1)$$

The filled circles in Fig. 3A give the van Hove correlation function for  $\tau = 1$  s obtained in a passive actin network without myosin. It is to be noted that  $P(\Delta x(\tau))$  is obtained by dividing the frequency histogram of  $\Delta x(\tau)$  by the product of the total number of samples and the binning size of  $\Delta x$  in units of  $\mu\text{m}$ . Since the fluctuations are purely thermal and this lag time lies in the network's elastic plateau regime, *i.e.*, there are no relaxation kinetics, the distribution of the observed trajectories was almost Gaussian. The solid curve in the same figure is a fitted Gaussian function. The slight deviation from the Gaussian fit observed in the tails of the distribution likely results from the heterogeneously cross-linked structure of the network.<sup>21</sup> A similar effect is

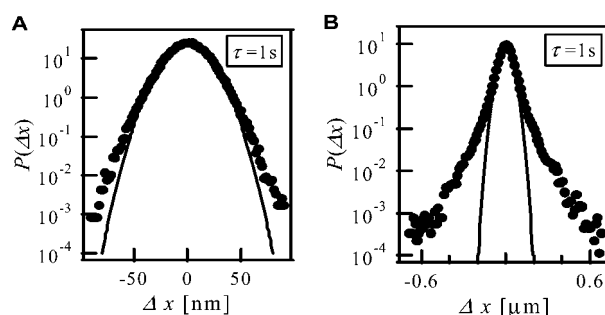


**Fig. 3** (A) Ensemble-averaged van Hove correlation function of probe particles in cross-linked actin networks without myosin (solid circles). The distribution approximately agrees with a Gaussian (solid curve). The slight deviations in the tails of the distribution are due to the heterogeneous cross-linking structure. (B) Ensemble-averaged van Hove correlation function of probe particles in an active gel (solid circles). While the centre of the distribution is still well fitted by a Gaussian, the large deviations in the tails of the distribution reflect overall non-Gaussian behavior.

observed in passive, slowly relaxing (*i.e.*, *glassy*) systems due to dynamic heterogeneities.<sup>22</sup> On the other hand, in active gels, the van Hove correlation function for the same lag time  $\tau = 1$  s shows a substantial deviation from Gaussian, as shown in Fig. 3B. Here, the solid curve is the fitted Gaussian to the central part of the distribution, which strongly deviates from the measured values (filled circles) at the tails (*i.e.*, for large displacements).

In order to quantify the deviation of the van Hove correlation function from a Gaussian distribution, we measured the one-dimensional non-Gaussian parameter (NGP)<sup>23</sup> which is defined as

$$\text{NGP} = \frac{\langle \Delta x(\tau)^4 \rangle}{3 \langle \Delta x(\tau)^2 \rangle^2} - 1, \quad (2)$$

where  $\langle \dots \rangle$  indicates the ensemble average. This dimensionless parameter, which can be positive or negative, vanishes for a Gaussian distribution, and can thus be taken to represent the degree of non-Gaussianity of a distribution. In a homogeneous system in equilibrium, this parameter takes finite values only when there exists some relaxation kinetics whose characteristic time is similar to the lag time.<sup>23</sup> In contrast, there is no *a priori* reason to expect a Gaussian distribution for athermal fluctuations.<sup>24</sup> In Fig. 4, the time-dependencies of the non-Gaussian parameter in active and passive networks (without myosin) are shown as curves and filled circles, respectively. In passive networks, the non-Gaussian parameter was always approximately zero, as expected. On the other hand, in active gels it clearly takes positive  $O(1)$  values, in a manner that depends on the lag time: after initially increasing for small lag times (in most datasets), it reaches a maximum value around  $\tau \approx 10$  s, and then decreases towards zero as  $\tau$  increases.

## Discussion

The circles in Fig. 5A and B give the van Hove correlation function obtained in active gels for  $\tau = 0.033$  s and  $\tau = 3.33$  s,

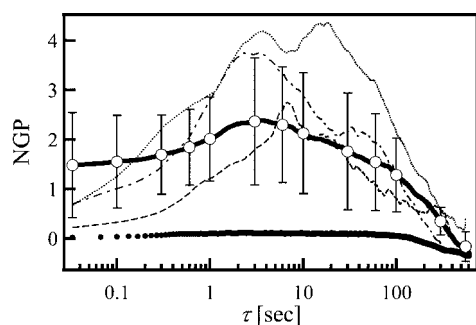


**Fig. 4** Solid curve and open circles show the lag time dependence of the non-Gaussian parameters for probe particle fluctuations observed in active gels. Error bars given for several representative lag times show the standard deviation estimated from 6 experiments. Filled circles show the same in passive gels (cross-linked actin without myosin). In the passive gel, the NGP is always approximately zero. In contrast, in active gels, the NGP is small or zero at short and long lag times and takes finite values at intermediate times. Some of the data for active gels with small athermal fluctuations exhibit clear decreasing behavior at short lag times (broken lines).

respectively. The distributions of thermal fluctuations measured in passive gels for the same lag times are also shown in these figures as dotted lines. At the shortest timescale accessible to video microscopy ( $\tau = 0.033$  s, at a sampling rate of 30 Hz), the centre of the distribution closely matches the equivalent thermal data. From this, one might infer that this region of the distribution predominantly originates from thermal fluctuations. The deviation from the thermal data, and indeed from the Gaussian form as apparent in the tails of the distribution, might be therefore attributable to athermal fluctuations.

In our prior work, however, we carried out active micro-rheology, which directly measures the response of colloidal particles to externally applied forces, on similar systems, and found that the active gels are significantly stiffened compared to the corresponding passive gels (the same sample but without myosin).<sup>3</sup> In active gels, myosin mini-filaments act as ‘active’ cross-linkers, albeit completely outnumbered by the static cross-links based on the bindings between neutravidin and biotinylated actins. The extra tension applied to the network due to the myosin force generations stiffens the actin network *via* the nonlinear response mechanism typical to semi-flexible polymers such as actin.<sup>3,25</sup> The actual contribution of thermal fluctuations

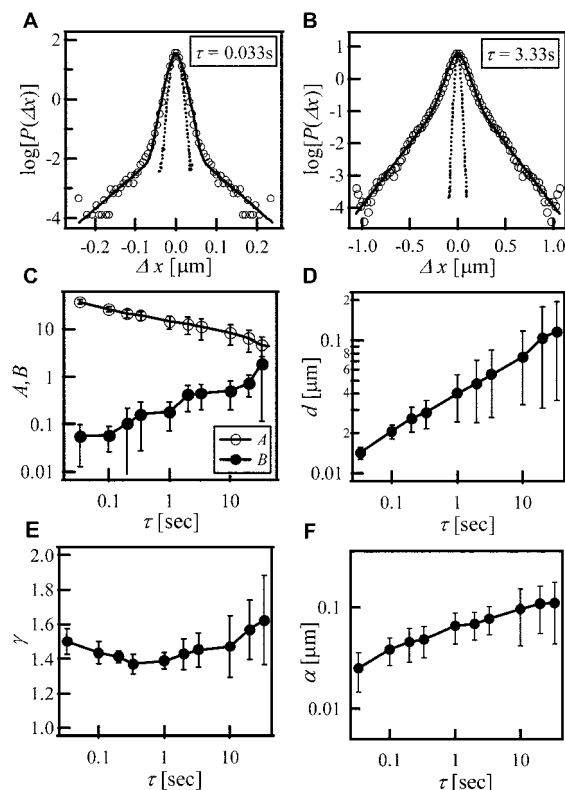


**Fig. 5** (A and B) The open circles indicate normalized van Hove correlation functions for probe particles in an active gel at  $\tau = 0.033$  s and 3.33 s, respectively. The dotted curves show the distribution of thermal fluctuations observed in an actin network without myosin at the same lag time. The solid curves show fits of eqn (4) to the van Hove correlation functions. (C–F) Average of lag-time dependence of fitting parameters. Bars show the standard deviations estimated from 6 experiments.  $B$  increases with lag time while  $\alpha$  is only moderately dependent on  $\tau$ .

in these actively stressed networks should therefore be much smaller than the dotted lines in Fig. 5A and B.

The non-Gaussian tails show approximately linear dependence in a single-logarithmic plot, corresponding to an exponential shape. The distribution obtained for the longer lag time of  $\tau = 3.33$  s is broader both in the central and the tail regions, as shown in Fig. 5B. The central part of the distribution, although taking an approximately Gaussian shape, is much larger than the thermal distribution at the same lag time. Furthermore, the tail distribution still shows an approximate exponential dependence with a similar slope to the shorter lag time, but with a larger magnitude.

This observed behavior can be qualitatively explained in terms of the competing roles of thermal and athermal fluctuations, and the broad distribution of the amplitudes of athermal fluctuations resulting from the broad range of probe–myosin separations. As reported in prior studies<sup>3,26</sup> and also discussed in this article, myosin mini-filaments link different actin filaments and drive them relative to each other (Fig. 1). As schematically shown in Fig. 6, the force or run length of myosin mini-filaments along each actin filament can be modeled to increase (approximately) linearly from zero, until it abruptly returns to zero after a stochastically occurring detachment (denoted by the arrows in Fig. 6). This localized motor-driven perturbation then propagates through the material, according to its dispersion properties, before imparting a corresponding displacement on a probe particle. Such behavior was directly observed in the probe particle trajectories, where once in a while a probe particle is pulled gradually in one direction and then rapidly moves back to its original position (see the movies in the ESI†).

Assuming linear response, the total measured displacement of the probe particles is the sum of thermal white noise, and athermal fluctuations due to myosin activity both near to and far from the probe. Furthermore, for each myosin mini-filament, perturbations take the form of both slow, gradual increments and sudden release events. Thus the resultant spectrum of probe displacements depends on factors such as the spatial distribution

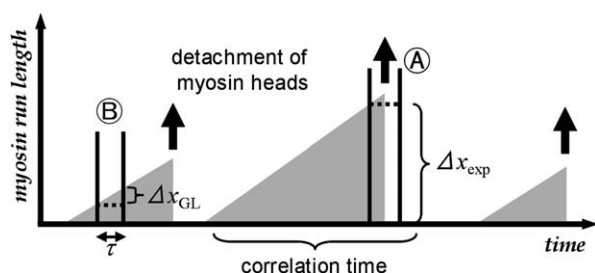


**Fig. 6** Illustration of the time dependence of force generation, or equivalently the run length of myosin mini-filaments along the interacting actin filaments, that increases gradually from zero to some maximum value and abruptly drops down to zero. The longer the correlation time for force generation, the longer the myosin's run length. Upward arrows indicate detachments of myosin heads. If the displacement of particles was sampled between the points which include a myosin detachment event, as shown in (A), the distribution of displacements  $\Delta x_{\text{exp}}$  is found to be exponential, implying that the myosin detachment is a Poisson process. For short lag times, the displacement of particles sampled at times where myosin is generating force continuously, as shown in (B), contributes to Gaussian-like central part of the distribution,  $\Delta x_{\text{GL}}$ .

of the motors, their individual motile properties, and the gel's viscoelasticity. The key new ingredient in the present study is that we consider the whole spectrum of spherical probe displacements rather than just the mean squared value, suggesting the possibility that suitable analysis will permit simultaneous determination of a variety of quantities related to active gels.

It is intuitive that motor activity near probe particles will induce larger displacements than those far away. Indeed, since the timescales accessible in this study corresponded to the elastic plateau of the actin network,<sup>27</sup> we can be more precise: treating the active stress generated by a myosin mini-filament as a (point-size) force dipole with a frequency-dependent moment  $\kappa$ , then the  $2m^{\text{th}}$  moment due to all motors in a range  $r$  from the center of a probe of radius  $a < r$  is

$$\langle u^{2m} \rangle \sim c \left( \frac{\kappa}{G} \right)^{2m} \left( \frac{1}{a^{4m-3}} - \frac{1}{r^{4m-3}} \right). \quad (3)$$

Here,  $c$  is the number density of myosin mini-filaments and  $G$  is the shear modulus of the actin network. This result, which is a straightforward generalization of the dimensional arguments discussed in ref. 28 and 29, is valid for an infinite isotropic elastic continuum and stems from the  $\sim 1/r^2$  decay of displacement with distance from the dipole.<sup>30</sup> This expression explicitly demonstrates that higher moments of the distribution are increasingly dominated by motors close to the probes, in the sense that 50% of the total contribution to the  $2m^{\text{th}}$  moment comes from motors within a range  $a < r < 2^{1/(4m-3)}a$ . Thus, 50% of the second moment comes from motors in the range  $a < r < 2a$ , 50% of the fourth moment from  $a < r < 1.15a$ , 50% of the sixth moment from  $a < r < 1.08a$ , and so on. Since higher moments describe statistics further into the tails of the distribution, this leads to the conclusion that the tail will be controlled by a small number of motor proteins. Indeed, we argue below that the measured exponential tail is due to the single, nearest motor protein to each probe particle.

Still assuming we are in the elastic plateau regime, the frequency dependence of the formula in eqn (3) stems solely from the temporal properties of the force dipoles, which derives from the repetitive pattern of gradual growth followed by stochastic release described in Fig. 6. It is from this process that the exponential tail of the distribution derives, as we now explain. As has been observed in single molecule studies,<sup>31,32</sup> we assume that detachment events are random and independent of time, so that these events obey Poisson statistics. The duration of contiguous motor activity for each event, *i.e.* the time before release, then follows an exponential distribution. Thereby the displacement due to the detachment, which is approximately proportional to the duration of the growth phase, also follows an exponential distribution. Therefore, the largest probe displacements that lie in the tail of the distribution will correspond to the release events of the myosin mini-filaments closest to the probe particle.

To characterize both the spatial and temporal aspects of active gels, we fit the normalized van Hove correlations calculated for active gels to the following four-parameter form, consisting of a Gauss-like distribution for the central part and an exponential distribution for side slope,

$$f(x) = A \exp[-(x/d)^\gamma] + B \exp[-x/\alpha]. \quad (4)$$

Here,  $d$  and  $\alpha$  are the characteristic distances for each distribution, and  $\gamma > 1$  is an empirical parameter which generalizes a Gaussian distribution;  $\gamma = 2$  when the central region is a standard Gaussian. Using  $\int_{-\infty}^{\infty} f(x)dx = 1$ ,  $B$  can be written as

$$B = \frac{1}{2\alpha} \left\{ 1 - 2dA\Gamma \left( 1 + \frac{1}{\gamma} \right) \right\} \quad (5)$$

Thus, fits to normalized van Hove correlation functions are carried out with four free parameters in total. The solid lines in Fig. 5A and B are the fitted curves to eqn (4). We calculated the van Hove correlation functions for various lag times and hence obtained the lag-time dependence of the fitting parameters ranging from  $\tau = 0.033$  s to  $\tau = 33.3$  s. Van Hove correlations for longer lag times become closer to a single Gauss-like distribution which is substantially different from eqn (4). The results for all fitting parameters are shown in Fig. 5C–F.

The empirical parameter  $\gamma$  for the active gels is approximately 1.5, similar to that in passive gels, which maybe coincidental (see ESI†). The monotonous increase of  $d$  in the active gel is in contrast to the constant plateau at  $d \approx 0.02$   $\mu\text{m}$  for the passive gel case (Fig. C in the ESI†). The monotonous growth of  $B$  for short lag times can be explained since the possibility to observe the sudden release events of myosins should initially increase linearly with time  $B \approx \tau$ . The fitted value  $\alpha$  gives a lower estimate for the mean run length of myosin mini-filaments, which from Fig. 5C is  $\sim 100$  nm, and which is constant (or weakly varying) with the lag time (the slight variation may be an artefact of the finite fitting window for the shortest lag times).

Turning to the lag-time dependence of the NGP shown in Fig. 4, it is already known that for high frequencies, athermal fluctuations are negligible compared to thermal fluctuations.<sup>3</sup> Thus, for extremely small lag times, the NGP should take the same value as passive gels, *i.e.*  $\sim 0$ . Although this regime cannot be clearly observed with video microrheology due to the slow sampling rate, some of the data shown in Fig. 4 are suggestive of a small (or zero) NGP for frequencies exceeding our window. For the intermediate lag times that video microrheology can access, athermal fluctuations begin to dominate over thermal fluctuations as we have described previously. Since the distribution of the athermal fluctuations is intrinsically non-Gaussian, the NGP is non-zero. For longer timescales, although athermal fluctuations are still dominant over thermal fluctuation, the NGP gradually approaches zero as shown in Fig. 4. As many independent events contribute to the central region, *i.e.*, small total displacements, the central limit theorem tells us that the resulting distribution should again be Gaussian, even though such fluctuations are non-equilibrium. The data shown in Fig. 4 qualitatively agree with the behavior described above.

It is therefore possible to expect that  $B$  reaches its maximum at a lag time which is similar to the time when the NGP starts to decrease ( $\sim 10$  s); both give a measure of the total time in between release events. But it is not easy to extract the time from Fig. 5C due to the substantial noise for large lag times. This noise results from the inability of the fitting function, eqn (4), to clearly delineate the central region from the tail for large  $\tau$ , plus the fact that, given a finite set of data points in real time, there will be fewer combinations for large lag times than short ones and

correspondingly poorer statistics. Taking an estimated value of 10 s from Fig. 4 and 5C and combining this with the mean run-length of 100 nm, we infer a run velocity of  $\sim 10$  nm s<sup>-1</sup> for attached, active myosin mini-filament head groups, although we stress this should be regarded as an order-of-magnitude estimate.

These fundamental characteristics of motor activity have been obtained in single molecule studies in recent years<sup>17,18,31,32</sup> but could not be observed in cytoskeletons or in cells so far. Analyzing the small displacements of the probe particles, on the other hand, is more complicated, as it derives from a number of sources: thermal fluctuations, the gradual build-up and release events of motors far from the probe particles, and, for short lag times, the gradual build-up of stresses due to motors close to the probes. For large lag times comparable to the correlation time for motor activation cycles, even these build-up intervals contribute to the tails of distribution. The resulting regime in the van Hove correlation function is therefore approximately Gaussian because many independent events (with finite variance) contribute, so the central limit theorem applies; it does *not* apply in the tail since only a few (or one) motors contribute to this regime, so instead we observe the bare exponential distribution of a single active motor complex.

## Materials and methods

### Sample preparation

Unlabeled G-actin and myosin II were prepared from rabbit skeletal muscle according to published methods.<sup>33</sup> Biotinylated actin (Cytoskeleton, Inc.) and neutravidin (Invitrogen, used as a cross-linker) were premixed and left over one hour on ice and then mixed with G-actin stored in G-buffer (2 mM: Tris-Cl, 0.2 mM: CaCl<sub>2</sub>, 0.5 mM: DTT, 0.2 mM: ATP, pH 7.5). The ratios were G-actin:biotinylated actin:neutravidin = 180 : 5 : 2. Then, we mixed adequate amounts of 1  $\mu\text{m}$  silica particles (Polysciences, Inc.) as probe particles to the actin solution. Myosin II in buffer (0.6 mM: KCl, 50 mM: KH<sub>2</sub>PO<sub>4</sub>, pH 6.5) was diluted into F-buffer (2 mM: HEPES, 2 mM: MgCl<sub>2</sub>, 50 mM: KCl, 1 mM: EGTA, 1 mM: ATP, pH 7.5) with ATP. The proteins were stored at  $-80$  °C. Finally, we mixed G-actin solution and myosin in the F-buffer. The total concentrations of actin and myosin were 1 mg ml<sup>-1</sup> and 170 nM, respectively. After mixing, samples were infused into the sample chamber (inner scales were 20 mm  $\times$  5 mm  $\times$  200  $\mu\text{m}$ ) made from a microscope slide glass and a cover slip and double-sided sticky tape.

Several samples with slightly different initial ATP concentrations ranging from 2 mM to 5 mM were prepared at once. Several hours after preparation, athermal fluctuations were observed in samples with initial ATP concentrations of 3.5–4 mM. The samples with lower ATP concentrations superprecipitated before the formation of a stably cross-linked actin network. Samples with higher ATP concentrations did not show athermal fluctuations till the end of the experiment.<sup>3</sup>

### Experiments

We recorded the microscope (Nikon TE-2000) images taken at the centre of the sample chamber directly to a PC at a sampling rate of 30 Hz. Probe particles were tracked using a custom-made LabVIEW program. Their center-of-mass positions were

calculated, and we obtained a time-sequence as a 2-dimensional array;  $x_n(t)$  and  $y_n(t)$  with  $n$  the particle number.

In Fig. 3, the van Hove correlation functions were calculated as the superposition of  $P(\Delta x(\tau))$  and  $P(\Delta y(\tau))$ , since overall fluctuations were isotropic. In order to have a better fit of eqn (4) to the van Hove correlation, the van Hove correlation functions in Fig. 5 were calculated as  $\{P(\Delta x(\tau)) + P(\Delta y(\tau)) + P(-\Delta x(\tau)) + P(-\Delta y(\tau))\}/2$ . Since the probability to have large displacements of particles can be extremely small, the binning size for larger displacements was systematically increased so that there were no bins with too small a number of counts. Also, since a straight least-squares fit would give too much weighting to points in the centre of the distribution at the expense of those in the tail, the logarithm of the van Hove correlation was fitted to the logarithm of the fitting function.

## Conclusions

In this study, we obtained the van Hove correlation functions  $P(\Delta x(\tau))$  of the displacement of colloidal particles dispersed in an active gel, which addresses both the spatial and temporal characteristics of athermal fluctuations. The mean squared displacements  $\langle \Delta x(\tau)^2 \rangle$ , or equivalently the auto-power spectrum  $C(\omega) = \int \langle x(\tau)x(0) \rangle \exp(i\omega\tau) d\tau$ , of the probe particles' motion can be calculated from  $P(\Delta x(\tau))$  as  $\langle \Delta x(\tau)^2 \rangle = \int (\Delta x(\tau))^2 P(\Delta x(\tau)) d(\Delta x)$ . In conventional micro-rheology,  $\langle \Delta x(\tau)^2 \rangle$  or  $C(\omega)$  is sufficient to deduce the viscoelastic properties of the surrounding material, if it is in equilibrium.

The full  $P(\Delta x(\tau))$  contains additional information regarding the distribution of athermal activity. We have demonstrated here that the van Hove correlation function of an actin–myosin active gel can be fitted to a sum of a Gaussian-like and an exponential distribution. The Gaussian-like central region derives from the action of many motor proteins far from the probes, whereas the exponential tail corresponds to a single force dipole close to the probe particle. By analyzing the tail, we were able to therefore provide an estimate of motor head velocity along the filament. A solvable theoretical model will confirm these qualitative trends and highlight the competing roles of thermal and athermal fluctuations at the shortest lag times accessible to video tracking.<sup>34</sup> We expect that further modeling of the non-Gaussian aspects of the van Hove distribution will permit a more precise and thorough characterization of the effects of non-equilibrium force generators in cytoskeletal networks, and will aid in our understanding of the mechanics of living cellular cytoskeletons.

## Acknowledgements

This work was supported by KAKENHI, a Program for the Improvement of the Research Environment for Young Researchers from SCF (Japan), and by the Asahi Glass Foundation and the Sumitomo Foundation (Japan). D.A.H. was funded by the European Network of Excellence “SoftComp”. C.F.S. was supported by the Center for the Molecular Physiology of the Brain (CMPB), and by the Sonderforschungsbereich

SFB 755, funded by the Deutsche Forschungsgemeinschaft (DFG).

## References

- 1 L. D. Landau, E. M. Lifshits and L. P. Pitaevskii, *Statistical Physics*, Butterworth-Heinemann, Oxford, Boston, 1980.
- 2 A. W. C. Lau, B. D. Hoffman, A. Davies, J. C. Crocker and T. C. Lubensky, *Phys. Rev. Lett.*, 2003, **91**, 198101.
- 3 D. Mizuno, C. Tardin, C. F. Schmidt and F. C. MacKintosh, *Science*, 2007, **315**, 370–373.
- 4 L. A. Hough and H. D. Ou-Yang, *Phys. Rev. E: Stat., Nonlinear, Soft Matter Phys.*, 2002, **65**, 021906.
- 5 D. Mizuno, D. A. Head, F. C. MacKintosh and C. F. Schmidt, *Macromolecules*, 2008, **41**, 7194–7202.
- 6 D. Mizuno, Y. Kimura and R. Hayakawa, *Phys. Rev. Lett.*, 2001, **8708**, 088104.
- 7 T. G. Mason and D. A. Weitz, *Phys. Rev. Lett.*, 1995, **74**, 1250–1253.
- 8 B. Schnurr, F. Gittes, F. C. MacKintosh and C. F. Schmidt, *Macromolecules*, 1997, **30**, 7781–7792.
- 9 F. Gittes, B. Schnurr, P. D. Olmsted, F. C. MacKintosh and C. F. Schmidt, *Phys. Rev. Lett.*, 1997, **79**, 3286–3289.
- 10 D. Mizuno, R. Bacabac, C. Tardin, D. Head and C. F. Schmidt, *Phys. Rev. Lett.*, 2009, **102**, 168102.
- 11 D. H. Boal, *Mechanics of the Cell*, Cambridge University Press, Cambridge, UK, New York, 2002.
- 12 D. Bray, *Cell Movements: from Molecules to Motility*, Garland Pub., New York, 2001.
- 13 E. Paluch, C. Sykes, J. Prost and M. Bornens, *Trends Cell Biol.*, 2006, **16**, 5–10.
- 14 A. B. Kolomeisky and M. E. Fisher, *Annu. Rev. Phys. Chem.*, 2007, **58**, 675–695.
- 15 J. Y. Xu, A. Palmer and D. Wirtz, *Macromolecules*, 1998, **31**, 6486–6492.
- 16 J. Liu, M. L. Gardel, K. Kroy, E. Frey, B. D. Hoffman, J. C. Crocker, A. R. Bausch and D. A. Weitz, *Phys. Rev. Lett.*, 2006, **96**, 118104.
- 17 T. Funatsu, Y. Harada, M. Tokunaga, K. Saito and T. Yanagida, *Nature*, 1995, **374**, 555–559.
- 18 K. Kitamura, M. Tokunaga, A. H. Iwane and T. Yanagida, *Nature*, 1999, **397**, 129–134.
- 19 F. Gittes and C. F. Schmidt, *Methods Cell Biol.*, 1998, **55**, 129–156.
- 20 T. Hayashi and K. Maruyama, *J. Biochem.*, 1975, **78**, 1031–1038.
- 21 M. T. Valentine, P. D. Kaplan, D. Thota, J. C. Crocker, T. Gisler, R. K. Prud'homme, M. Beck and D. A. Weitz, *Phys. Rev. E: Stat., Nonlinear, Soft Matter Phys.*, 2001, **6406**, 061506.
- 22 P. Chaudhuri, L. Berthier and W. Kob, *Phys. Rev. Lett.*, 2007, **99**, 060604.
- 23 A. Rahman, *Phys. Rev. Sect. A*, 1964, **136**, A405–411.
- 24 C. P. Brangwynne, G. H. Koenderink, F. C. MacKintosh and D. A. Weitz, *Phys. Rev. Lett.*, 2008, **100**, 118104.
- 25 G. H. Koenderink, Z. Dogic, F. Nakamura, P. M. Bendix, F. C. MacKintosh, J. H. Hartwig, T. P. Stossel and D. A. Weitz, *Proc. Natl. Acad. Sci. U. S. A.*, 2009, **106**, 15192–15197.
- 26 D. Humphrey, C. Duggan, D. Saha, D. Smith and J. Kas, *Nature*, 2002, **416**, 413–416.
- 27 F. Gittes and F. C. MacKintosh, *Phys. Rev. E: Stat. Phys., Plasmas, Fluids, Relat. Interdiscip. Top.*, 1998, **58**, R1241–R1244.
- 28 D. A. Head and D. Mizuno, *Phys. Rev. E: Stat., Nonlinear, Soft Matter Phys.*, 2010, **81**, 041910.
- 29 F. C. MacKintosh and A. J. Levine, *Phys. Rev. Lett.*, 2008, **100**, 018104.
- 30 L. D. Landau, E. M. Lifshits, A. D. M. Kosevich and L. P. Pitaevskii, *Theory of Elasticity*, Pergamon Press, Oxford, New York, 1986.
- 31 S. M. Block, L. S. B. Goldstein and B. J. Schnapp, *Nature*, 1990, **348**, 348–352.
- 32 Z. H. Wang, S. Khan and M. P. Sheetz, *Biophys. J.*, 1995, **69**, 2011–2023.
- 33 L. W. Cunningham, D. W. Frederiksen and R. B. Vallerie, *Structural and Contractile Proteins*, Academic Press, New York, 1982.
- 34 D. Head, et. al, under preparation.